AN OPTIMISATION PROCEDURE FOR PROPELLER SELECTION FOR DIFFERENT SHAFT INCLINATIONS

Reference NO. IJME 809, DOI: 10.5750/ijme.v164iA3.809

M Tadros, Centre for Marine Technology and Ocean Engineering (CENTEC), Instituto Superior Técnico, Universidade de Lisboa, Portugal. Department of Naval Architecture and Marine Engineering, Faculty of Engineering, Alexandria University, Egypt, **M Ventura**, Centre for Marine Technology and Ocean Engineering (CENTEC), Instituto Superior Técnico, Universidade de Lisboa, Portugal and **C Guedes Soares**, Centre for Marine Technology and Ocean Engineering (CENTEC), Instituto Superior Técnico, Universidade de Lisboa, Portugal.

E-mail: c.guedes.soares@centec.tecnico.ulisboa.pt
Corresponding Author: C Guedes Soares

KEY DATES: Submitted: 22/11/21; Final acceptance: 20/12/22; Published: 31/01/23

SUMMARY

In this paper, a propeller optimisation model is presented to find the optimum propeller geometry and the gearbox ratio for different propeller shaft angles while minimizing the amount of fuel consumed at a given speed and complying with the proposed constraints' limitations. The developed model couples several simulation software where the application programming interface facilitates data processing to achieve the optimum design based on optimisation procedures. A fishing vessel is selected as a case study to perform the numerical simulation. A comparison study is conducted between the optimized propellers at different inclination angles of the propeller shaft among different propeller blades. Bar chart and box and whisker plot are the two techniques considered to visualize the computed data. The results conclude that the optimized propeller with a high number of blades and a small inclination angle (2 degrees) can operate at the engine operating point as in a horizontal propeller shaft, which is considered the most efficient from the theoretical point of view.

KEYWORDS

Fishing vessel; Optimisation model; Minimum fuel consumption; Inclined propeller shaft.

NOMENCLATURE

Symbol	Definition
1D	One dimensional
3D	Three-dimensional
API	Application programming interface
B	Breadth (m)
B	Bore (mm)
BEM	Boundary element method
$BSFC$	Brake specific fuel consumption (g/kW.h)
$c(x)$	Inequality constraints
CA	Correlation-allowance
CAD	Computer-aided design
$c_{eq}(x)$	Equality constraints
CFD	Computational fluid dynamics
C_n, S_n, t_n, u_n, v_n	Constants
CPP	Controllable pitch propeller
D	Diameter (m)
dC_F	Roughness contributions
DES	Detached eddy simulation
DoE	Design of experiments
EAR	Expanded area ratio (−)
$f(x)$	Objective function
FC	Fuel consumption (l/nm)
FEM	Finite element method
FPP	Fixed pitch propeller
$g(x)$	Static penalty function
GA	Genetic algorithm
GBR	Gearbox ratio (−)
GUI	Graphic user interface
IMO	International Maritime Organisation
J	Advance coefficient (−)
j	Number of constraints
K_Q	Torque coefficient (−)
K_T	Thrust coefficient (−)
L	Stroke (mm)
lb	Lower bounds
LWL	Length waterline (m)
n	Propeller speed (rps)
N	Propeller speed (rpm)
N_{max}	Rated speed (rpm)
NSGA-II	Non-dominated sorting algorithm II
P/D	Pitch diameter ratio (−)
P_B	Brake power (kW)
P_{max}	Rated power (kW)
Q	Torque (N.m)
R	Penalty function (−)
RANS	Reynolds-averaged Navier–Stokes equations
R_n	Reynolds number (−)

RSM	Response surface methodology
T	Draught (m)
T	Thrust (N)
ub	Upper bounds
V	Engine displacement (liter)
V_A	Advance speed (m/s)
V_S	Service speed (knot)
$V_{s\text{-}max}$	Maximum speed (knot)
x	Number of variables
Z	Number of blades (−)
Δ	Ship displacement (tonne)
μ	Coefficient of dynamic viscosity (−)
η_o	Open water efficiency (%)
ρ	Density (kg/m^3)

1. INTRODUCTION

The selection of each component of the marine propulsion system is an essential process to increase the system's efficiency (Zalacko et al., 2021), reduce the amount of fuel consumption and comply with the stringent regulations of the International Maritime Organisation (IMO) (Tadros et al., 2020b, Elkafas et al., 2021, Elkafas and Shouman, 2021). Besides the rapid technologies presented in the engine as a prime mover (Altosole et al., 2017, Tadros et al., 2019, Tadros et al., 2021b, Elkafas et al., 2021), the propeller is considered an important and influential part to transmit the brake engine power and give thrust to the ship (Carlton, 2012). Therefore, several pieces of research, either experimental or numerical, have been performed to achieve the maximum propeller efficiency by finding the optimal propeller geometry and at the same time ensuring the durability of the propeller by reducing cavitation problems (Arapakopoulos et al., 2019, Ekinci, 2011).

The horizontal propeller shaft is the most efficient from the theoretical point of view. In practice, the restricted engine room area and the ship stability in small and medium ships must pay attention to designers because it is essential not to leave enough empty spaces and thus limit the cargo spaces. Therefore, the inclination of the propeller shaft is an important parameter that is used in several designs. This technique can change the forces imposed on the marine propeller, affecting the propeller performance by reducing thrust and efficiency and increasing vibration and cavitation issues (Seyyedi et al., 2019). Peck and Moore (1973) and Peck (1974) wrote earlier papers to present the characteristics of a series of propellers among a range of shaft angles to evaluate the applicability of installing inclined propellers on-board. They measured both horizontal and vertical side forces as well as the hydrodynamic properties to ensure the propeller durability. The main interesting thing is that the inclined propeller may generate more forward thrust than the propeller attached to a horizontal shaft.

Like in horizontal propeller shaft, the primary purpose of the research is to study the behaviour of flow passing through the propeller and its effect on the propeller performance to select an appropriate propeller (Kaewkhiaw, 2020). Therefore, Gaggero et al. (2010), Gaggero and Villa (2018), Vlašić et al. (2018) and Kumar et al. (2021) used Reynolds-averaged Navier–Stokes equations (RANS) to compute the propeller performance and flow characteristics. The results show a good agreement with the experimental data. Also, Kim and Kinnas (2020) used RANS to study the induced pressures to reduce noise on-board. Paik et al. (2011) estimated cavitation levels based on erosion tests for an inclined propeller shaft to evaluate marine coatings. Aktas et al. (2016) presented a systematic procedure using experimental tests to study the performance of an inclined propeller and the corresponding cavitation issues. It has been shown that the inclination of the propeller shaft significantly affects propeller torque and efficiency, as well as cavitation and noise issues. Usta and Korkut (2018) applied the detached eddy simulation (DES) method to compute the hydrodynamic performance of a controllable pitch propeller (CPP). The calculated results show a good agreement with the experimental data.

Regarding the computational systems, different effective tools have been developed to estimate propeller performance throughout the years. Based on the performed experimental tests, van Lammeren et al. (1969) and Oosterveld and Van Oossanen (1975) used computers to present the Wageningen B-series in polynomial equations to be easily used in the preliminary stage of ship design. This series was widely used in predicting the propeller performance in different marine applications to fulfil the objective of several studies (Vettor and Guedes Soares, 2016, Ghaemi and Zeraatgar, 2021). This series was then extended to cover the performance of other types of propellers such as Wageningen C-and D-series (Dang et al., 2012).

Other series with different propeller profiles are presented in a polynomial way, such as the Gawn AEW (Blount and Fox, 1978) as well as the ducted Kaplan propellers (Oosterveld, 1970). This surrogate model helps the ship designers have a comprehensive overview of the required installed propeller as well as easily apply optimisation procedures to find the optimal propeller with maximum propeller efficiency (Radojčić, 1985, Suen and Kouh, 1999, Lee et al., 2010) and avoid cavitation (Gaafary et al., 2011). Also, multi-objective optimisation is coupled to the polynomial equations to verify several objectives as presented in (Benini, 2003, Tan et al., 2019, Mirjalili et al., 2015, Tadros et al., 2021a).

Computers are becoming faster, and the processing of data is performed automatically in a smooth way through several programming languages and techniques. Therefore, various commercial and open-source software packages are developed to compute the propeller performance in a detailed technique that is then exported to the manufacturer. The developed commercial software are PSP and CSPDP

from Marin (2020), Heliciel software from Heliciel (2019) and NavCad, PropCAD and PropElement software from HydroComp (2018). In addition, JBLADE developed by Silvestre et al. (2013), and OpenProp, developed by Epps et al. (2009), are friendly open-source codes with a graphic user interface (GUI). The performance of each software is improved, and a new updated version is issued every year to keep up with the fast-developing market due to the technological revolution. For instance, the quality of meshing in computer-aided design (CAD) model is improved as well as the way of exporting the 3D CAD model of the propeller to fit several extension files. Furthermore, facilitating this procedure assists the users in implementing the 3D CAD model into other software for further applications such as structure analysis using the finite element method (FEM) (Ye et al., 2019) and hydrodynamic analysis using computational fluid dynamics (CFD) (Nouri et al., 2018, Bekhit and Lungu, 2019, Bekhit et al., 2020).

The operation research technique is used to find the optimal solution for the propulsion system avoiding performing a manual interaction between the different computer programs. Thus, the application programming interface (API) becomes an essential way to be implemented into the software for smart and easy connections. Therefore, the desired software can be coupled to third-party software for further computations or programming environment to facilitate the importing and exporting of data as well as to provide flexibility in post processing the computed results. Before developing API, the software can generate a lot of computed data to study the relationship between the input and output variables. This process is called the design of experiments (DoE) and effectively supports decisions based on response surface methodology. Vesting and Bensow (2011) used the non-dominated sorting algorithm II (NSGA-II) to find the best propeller geometry based on CFD-generated data at maximum propeller efficiency while minimizing cavitation issues.

After using API, the software can be easily coupled to a third-party code. For instance, NavCad software, in its premium feature, can be coupled automatically to Matlab or Python environment through API code. This procedure allows the users to perform any kind of study according to their needs; for instance, MacPherson et al. (2016) coupled NavCad, as a propulsion simulation tool, and CAESES (2021) as an optimisation software to find the optimum hull form with a proper waterjet to increase ship speed. Tadros et al. (2021c) and Tadros et al. (2022a) coupled the same propulsion simulation tool and Matlab to find the optimal propeller geometry that achieves the minimum fuel consumption level at the ship's service speed. Also, Tadros et al. (2022b) considered the propeller cup to achieve the lowest level of fuel consumption and cavitation than the uncapped propeller. This study follows the same concept presented in (Tadros et al., 2019), where a 1D engine simulation optimisation model is developed to find the optimal parameters of a marine diesel engine.

OpenProp is another software already built-in Matlab environment to evaluate the propeller's performance in a 3D mode so that it can be easily adapted to be coupled to any of the optimisation methods in the same programming environment to find the optimal values of propeller geometry. Taheri and Mazaheri (2013) developed an optimisation model to optimize the geometry and maximize the efficiency of two types of propellers. Tadros et al. (2018a) adapted the code of OpenProp to be coupled with an optimizer integrated into Matlab to maximize the propeller efficiency by finding the optimum propeller geometry. Bacciaglia et al. (2021) developed the same concept of optimisation model to find the optimal solution of a CPP.

In general, optimizers are integrated into other commercial software to facilitate optimisation procedures. Pluciński et al. (2007) coupled boundary element (BEM) and FEM method with GA to maximize twist and optimize the material selection of a composite marine propeller. Gaggero et al. (2017) coupled the same software to increase ship speed by improving propulsive efficiency. Ansys (2018) has been used to design specific propellers to improve the blade shape of the existing propellers (Wärtsilä, 2021, MAN Energy Solutions, 2020) according to the requirement of the markets.

To conclude the previous points, Figure 1 shows the three main techniques to perform the propeller numerical simulation and achieve the optimum results. The three techniques are compared using the three-point Likert scale in terms of simulation time, time to build the initial code, accuracy of the computed results, and data processing among the code. The indicator is mentioned in the middle scale level and can vary more or less according to the application. The scale level is presented based on the authors' experience in the field to show that the operation research technique, either applied to DoE or directly coupled with the numerical code, offers advantages over the manual computation in terms of the accuracy of the results and processing of data. Therefore, more time is required to prepare and build the initial code and perform the simulation.

Based on the points presented above and by following the international regulator's recommendations to reduce fuel consumption during design and operation, this paper contributes to improving the fuel economy and thus the energy efficiency of ships by selecting an optimal propeller geometry at the corresponding operating point with minimum fuel consumption while considering the inclination of the propeller shaft angles. As a result, the model developed by Tadros et al. (2021c) is updated to

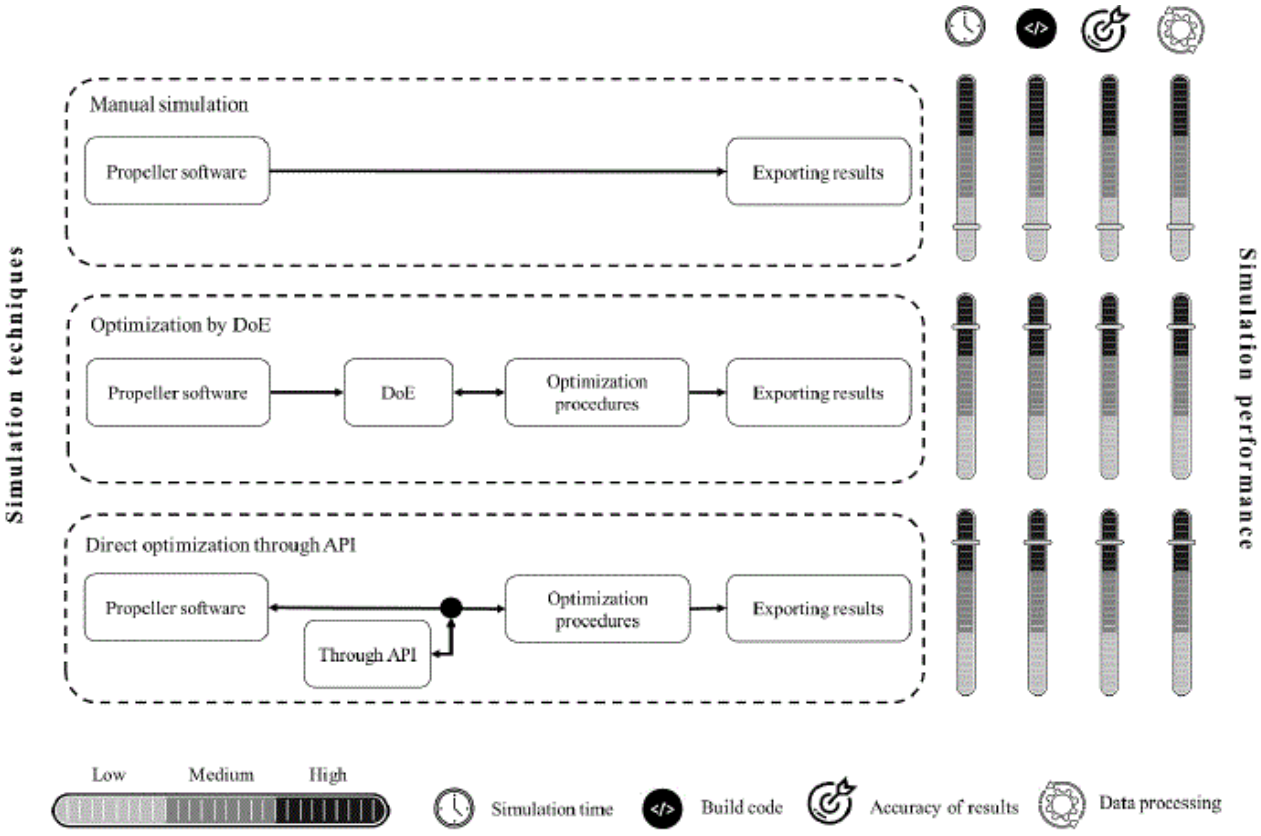

Figure 1. Comparison between different simulation techniques for propeller design.

implement the value of shaft angle and therefore find the optimum propeller geometry of a fishing vessel and its operating point with minimum fuel consumption in a fast way as well as complying with the limitations of cavitation and noise. Furthermore, a comparison study using visualized techniques is performed between the performance of the optimized propellers with different propeller blades among five degrees of the inclination angle of the propeller shaft. Thus, this model helps to decide on propeller selection during the preliminary stages of ship design.

The rest of the paper presents a general presentation of the ship and engine characteristics in section 2; section 3 presents an overview of the propeller optimisation model and the main equation used in the simulation. Finally, the computed results are discussed in section 4 and conclusions are presented in section 5.

2. MAIN SPECIFICATIONS OF THE FISHING VESSEL

In this study, a fishing vessel with 22 m is selected. This vessel is powered by one marine diesel engine with 200 kW (Solé Diesel, 2021), coupled to one fixed pitch propeller from B-series to propel the ship at 9 knots. The main characteristics of the vessel are presented in Table 1, while the engine characteristics are given in Table 2.

Table 1: Main characteristics of the fishing vessel.

Characteristics	Symbol	Unit	Value
Length waterline	LWL	m	21.98
Breadth	B	m	5.2
Draught	T	m	1.6
Displacement	Δ	tonne	104.3
Service speed	V_s	knot	9
Maximum speed	$V_{s\text{-}max}$	knot	10
Number of propellers	-	-	1
Type of propellers	-	-	FPP
Rated power	P_{max}	kW	200

Table 2: Main characteristics of marine diesel engine SDZ-280.

Characteristics	Symbol	Unit	Value
Engine builder	-	-	Solé Diesel
Bore	B	mm	108
Stroke	L	mm	130
Displacement	V	liter	7.145
Number of cylinders	-	-	6
Rated speed	N_{max}	rpm	2300
Rated power	P_{max}	kW	200

3. DESCRIPTION OF THE PROPELLER OPTIMISATION MODEL

3.1 GENERAL OVERVIEW

The optimisation model developed in this study couples NavCad software (HydroComp, 2018) and Matlab as a programming platform to analyze data. NavCad is a simulation tool used to compute hydrodynamic and propulsion systems based on numerical equations. The API implemented in NavCad (MacPherson et al., 2016) allows the software to be coupled to a third-party application, as mentioned in the literature review. This procedure facilitates the interaction between the different codes to achieve more accurate results in an appropriate simulation time. Figure 2 shows the schematic diagram used in this study to optimize the propeller performance.

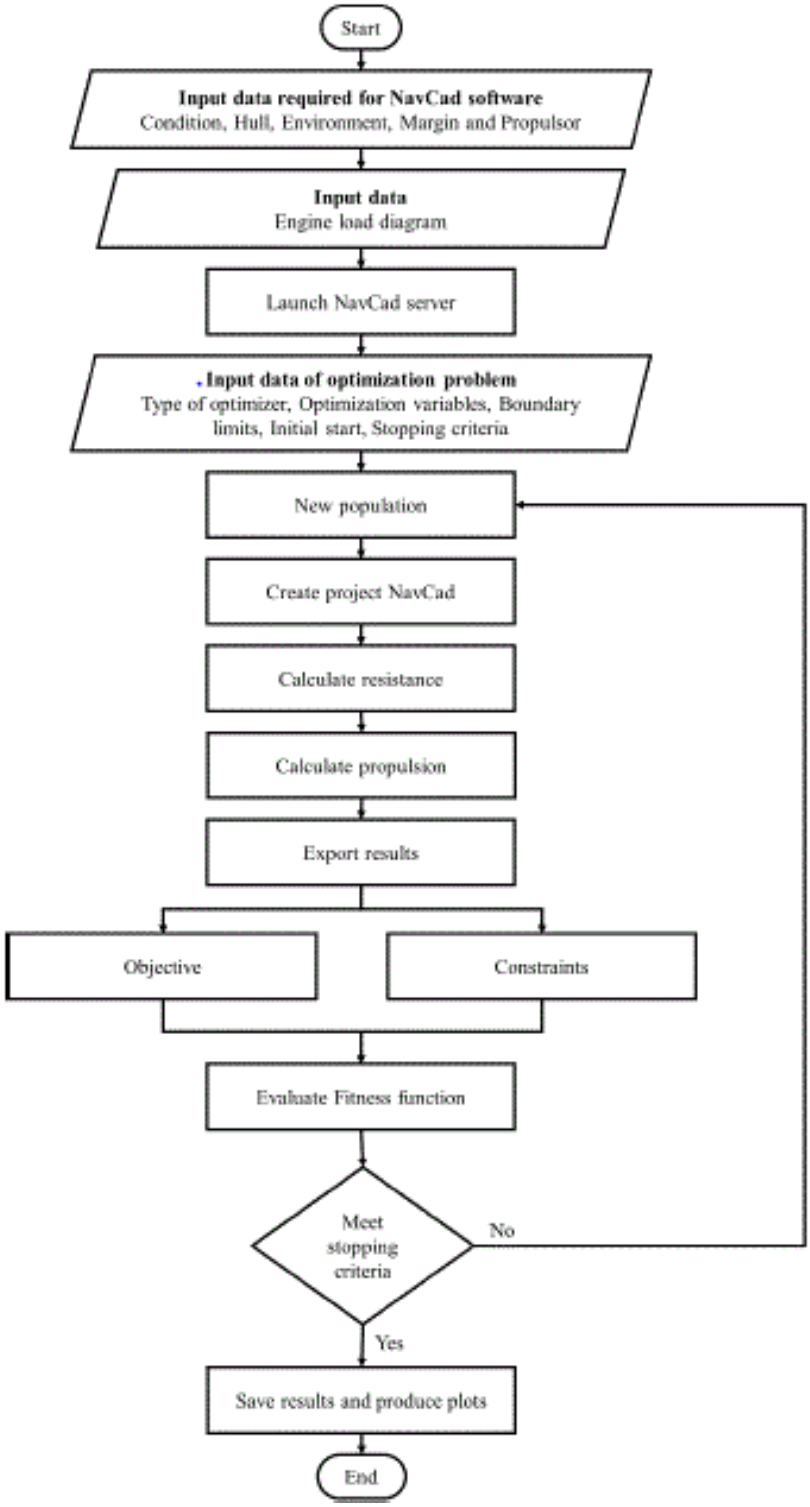

Figure 2. Schematic diagram of the propeller optimisation model.

3.2 PROPULSION SIMULATION SOFTWARE

The ship speeds and the main dimensions of the selected fishing vessel are defined in NavCad, including ship length and breadth at the waterline, ship draught, displacement and wetted surface. Then, according to the general arrangement of the ship, the centre of buoyancy and flotation, the maximum section and waterplane area, the immersion transom parameters, half entrance angle, and the shape factor of bow and stern are defined. To allow a feasible resistance prediction, 10% is added as a design margin to the added drag. Finally, all of this information is implemented to compute the ship resistance using the methods presented in (Holtrop, 1984, Holtrop, 1988) and comply with the recommendations of ITTC (2008), which affects the calculation of wave-making and residuary resistance, the prediction of correlation-allowance (*CA*) and roughness contributions (*dCF*).

The power prediction is computed based on the selected propeller series, the number of propellers and the number of blades in each propeller, the propeller geometry, the hub's immersion below the waterline, and the propeller shaft's inclination to the waterline. The driveline configuration of the propulsion system is selected, including the rated power and speed of the installed engine and the gear ratio. The efficiencies of the single-stage gearbox and a single screw propeller shaft line are specified by 97%. Once the parameters are defined in the software, the method of Holtrop and Mennen (1982) is chosen to compute the wake fraction and thrust deduction fraction for more realistic computation during the power prediction computation. Then the propeller characteristics and cavitation parameters are well calculated (Tadros et al., 2021a, Islam et al., 2022).

3.3 ENGINE LOAD DIAGRAM

The computed results from NavCad are passing through the data of the engine load diagram to compute the amount of fuel consumed at the engine operating point. The data of the engine load diagram are computed based on a developed 1D engine optimisation model (Tadros et al., 2020b), where the brake specific fuel consumption (*BSFC*) is computed for each engine operating point by finding the optimal engine configurations to achieve the minimum fuel consumption.

The results of this model are then converted to non dimensional polynomial equations using response surface methodology (RSM) to estimate the performance of other engines with the same behaviour. This conversion is performed based on response surface methodology as presented in (Tadros et al., 2018b, Tadros et al., 2020c) to fit the installed engine in the current case study.

3.4 SOFTWARE ARCHITECTURE

Matlab as a programming language is the main software used in data processing and in optimisation procedures.

It is used to prepare the input data for NavCad software and to export the computed results to be evaluated by the integrated optimizer through API.

A constrained nonlinear multivariable function (Fmincon) is selected as a fast and local optimizer used in several applications and suitable for finding high accurate results like any global optimizer based on initial start (Tadros et al., 2020a). It finds the optimal solution of the variables (x) within the lower (lb) and the upper (ub) bounds to minimize the objective function, $f(x)$, and to verify both inequality ($c(x)$) and equality constraints ($c_{eq}(x)$), as in equations (1)–(2). The interior-point is the optimisation algorithm selected as recommended by Matlab (The MathWorks Inc., 2018).

$$minimize \quad f(x) \tag{1}$$

$$\begin{aligned} subjected\ to: \ & c(x) \le 0 \\ & ceq(x) = 0 \\ & lb \le x \le ub \end{aligned} \tag{2}$$

For a given ship speed, the number of blades (Z), and the propeller shaft's inclined angle, the optimizer finds the optimal solution of the propeller geometry presented by diameter (D), pitch diameter ratio (P/D) and expanded area ratio (EAR), and gearbox ratio (GBR) by minimizing the fuel consumption using the equation (3) as considered the study's main objective and comply with the limitations of the constraints such as cavitation, strength, and noise.

$$FC_{l/nm} = \frac{BSFC \times P_B \times 1000}{\rho_{fuel} \times V_S} \tag{3}$$

where FC is the fuel consumption in litre per nautical mile, P_B is the brake power, ρ_{fuel} is the fuel density, and V_S is the ship speed.

The objective and the constraints are combined into the fitness function of the optimisation model as in the equation (4) as one of the techniques used for a complex problem. So, the value of the fitness function is minimized instead of the objective function, while the part of constraints will reach zero once the constraints are satisfied.

$$\begin{aligned} Fitness\ Function = & FC_{l/nm} \\ & + R\sum_{i=1}^{j} max(g_i(x), 0) \end{aligned} \tag{4}$$

where $g(x)$ is the static penalty function, j is the number of constraints and R is a penalty function.

3.5 PROPELLER SERIES

Wageningen B-series is the propeller series selected to perform the optimisation procedures. It has been chosen as one of the typical series used in the research field (Vettor and Guedes Soares, 2015, Vettor et al., 2016). The polynomial curves of this series are developed based on the open water analysis (Oosterveld and Van Oossanen, 1975) to be further used in ship design, as mentioned earlier in the literature review. Figure 3 shows a general plan of the Wageningen B-series. The number of blades in this propeller series varies from 3 to 7 blades. However, in this study, 4 to 6 blades are only considered in the simulation for a more realistic comparison. Table 3 shows the range of B-series parameters for a different number of blades. Based on the polynomial equations of the B-series, the advance coefficient (J), the thrust coefficient (K_T), torque coefficient (K_Q), and the open water efficiency (η_o) are the main parameters used to evaluate the propeller performance using the following equations:

$$K_T = \sum_{n=1}^{39} C_n (J)^{S_n} \left(\frac{P}{D}\right)^{t_n} (EAR)^{u_n} (Z)^{v_n} \tag{5}$$

$$K_Q = \sum_{n=1}^{47} C_n (J)^{S_n} \left(\frac{P}{D}\right)^{t_n} (EAR)^{u_n} (Z)^{v_n} \tag{6}$$

$$\begin{Bmatrix} K_T(R_n) \\ K_Q(R_n) \end{Bmatrix} = \begin{Bmatrix} K_T(R_n = 2\times10^6) \\ K_Q(R_n = 2\times10^6) \end{Bmatrix} + \begin{Bmatrix} \Delta K_T(R_n) \\ \Delta K_Q(R_n) \end{Bmatrix} \tag{7}$$

$$J = \frac{V_A}{nD} \tag{8}$$

$$K_T = \frac{T}{\rho n^2 D^4} \tag{9}$$

$$K_Q = \frac{Q}{\rho n^2 D^5} \tag{10}$$

$$\eta_o = \frac{K_T}{K_Q}\frac{J}{2\pi} \tag{11}$$

$$R_n = \frac{\rho n D^2}{\mu} \tag{12}$$

where R_n is the Reynolds number, V_A is the advance speed, n is the propeller speed, ρ is the density, μ is the coefficient of dynamic viscosity, T is the thrust and Q is the torque. C_n, S_n, t_n, u_n and v_n are constants that have different values in equations (5) and (6).

With the existence of an inclined propeller shaft, the numerical model follows the concepts presented in (Peck and Moore, 1973, Peck, 1974), as shown in Figure 4.

Table 3: Parameters of propeller series.

Parameter	Wagengein B-series
Number of blades	3 – 7
Blade area ratio	0.35 – 0.80 for 3 blades 0.40 – 1.00 for 4 blades 0.45 – 1.05 for 5 blades 0.50 – 0.95 for 6 blades 0.55 – 0.85 for 7 blades
Pitch/Diameter ratio	0.5 – 1.4
Advance coefficient	0.05 – 1.5

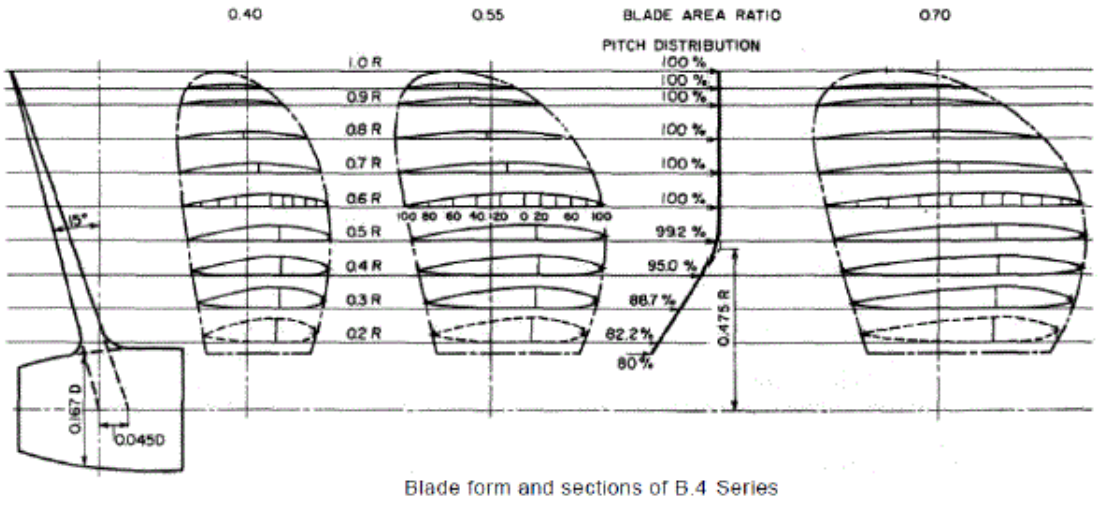

Figure 3. General plan of Wageningen B-series (HydroComp, 2018).

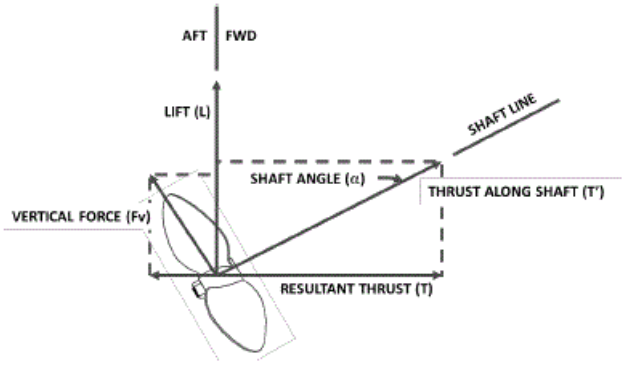

Figure 4. Force diagram along inclined propeller shaft (Peck, 1974).

The perpendicular forces to the shaft as well as the thrust and torque forces in the shaft are computed based on the basics of trigonometry, taking into account the cosine effects against horizontal and without any changes in the flow angle to the propeller.

Then, the cavitation issues are defined using the main three methods shown in Table 4, Keller, average loading pressure and average predicted back cavitation percentage. The reference of each method is mentioned as well as the limits to avoid cavitation problems. These limits are used as constraints of the optimisation model. The second constraint is the blade strength, and it is computed where the blade thickness must not be less than the computed minimum blade thickness. Finally, the tip speed is the last constraint that is used to evaluate the level of noise from the propeller and the limits of the tip speed are well defined in Table 4.

4. RESULTS AND DISCUSSION

The optimizer used in this study is a local optimizer, and it is essential to check the initial starting points during the optimizer configurations to achieve the minimum fuel consumption. Therefore, the numerical computation is performed for the horizontal propeller and at a higher blade number for several starting points as follows: (1) *LB*, (2) *(LB + UB)/4*, (3) *(LB + UB)/2*, (4) *(LB + UB)*3/4*, (5) *UB* and (6) random values. The fourth case shows the most suitable initial starting points for the optimizer in terms of fuel consumption, as shown in Table 5.

Once the initial point is selected, the optimisation procedures are applied to select the propeller geometry and the operational point at a defined number of blades (4, 5 and 6), and inclined shaft angles vary between 0 degrees (no inclination) and 5 degrees. The maximum value of the inclined propeller shaft (5 degrees) is selected according to the recommendations of ABS (2021) to eliminate the vibration issues. The optimisation model verifies all the constraints presented by the limitations of cavitation, noise and strength.

Before exporting the results, the simulation is performed again for all cases by setting the fifth initial starting point (*UB*), as common for better propeller performance. It has been found that the value of fuel consumption in the case of six-blade and the 2-degree inclination angle is lower than the optimum propeller in the same case while setting the fourth initial starting point. Therefore, the case with lower fuel consumption is considered while exporting the results.

Table 6 shows the computed results of the performance of the propeller among the different cases. While it is challenging to read these presented data, a dimensionless technique is applied to convert these numbers to be between 0 and 1, and a sensitivity analysis is presented using bar charts to be easily readable. Also, a box- and whisker-plot is applied to visualize parameters variation through their quartiles and identify the statistics parameters (McGill et al., 1978). As in Figure 6, the top and bottom of each box represent the upper and lower quartiles, respectively. The line inside each box represents the median. The top and bottom bars represent the maximum and minimum concentrations, respectively. The results are presented using the two visualization techniques in figures 5 to 34. The simulation case is named according to the value of

Table 4: The different constraints considered in the optimisation model.

Parameter	Method	Reference	Limits
Cavitation	Keller	Oosterveld and Van Oossanen (1975)	Greater than EARmin
	Average loading pressure	Burrill chart (Burrill and Emerson, 1963)	Less than 65 kPa
	Average predicted back cavitation percentage	Blount and Fox (1978)	Less than 15%
Strength	Minimum blade thickness	Oosterveld and Van Oossanen (1975)	Greater than minimum blade thickness
Noise	Tip speed	HydroComp (2018)	Less than 53 m/s for 3 and 4 blades Less than 46 m/s for 5, 6, 7 blades

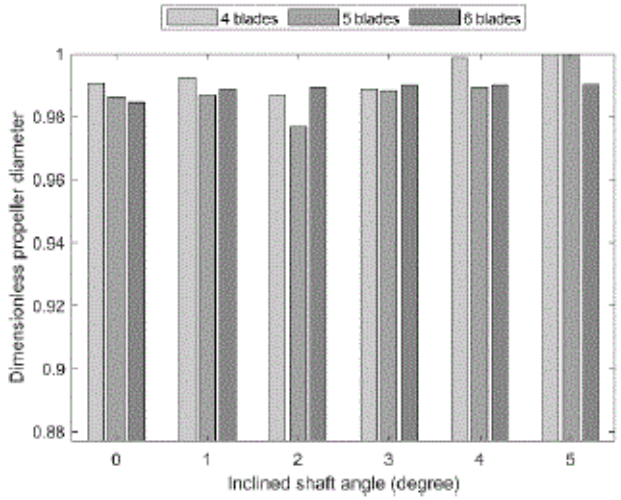

Figure 5. Dimensionless propeller diameter of different propeller blades at several inclined shaft angles.

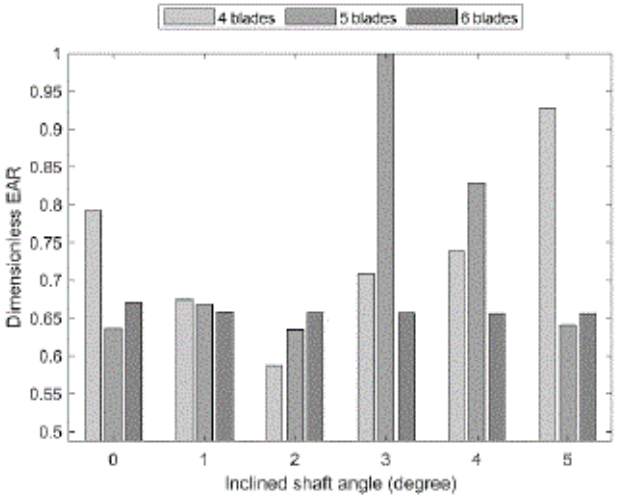

Figure 7. Dimensionless EAR of different propeller blades at several inclined shaft angles.

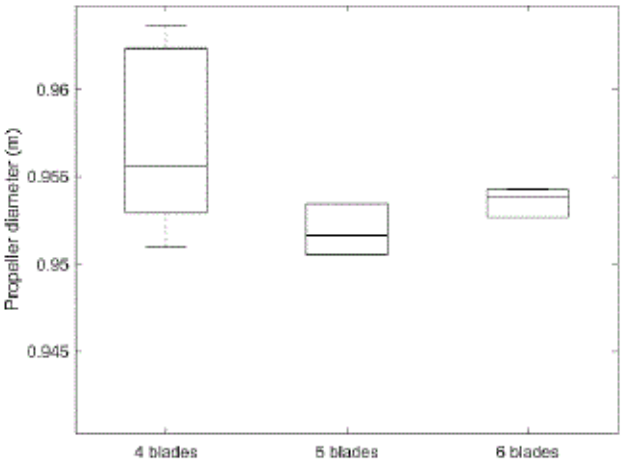

Figure 6. Box plot of propeller diameter among different propeller blades.

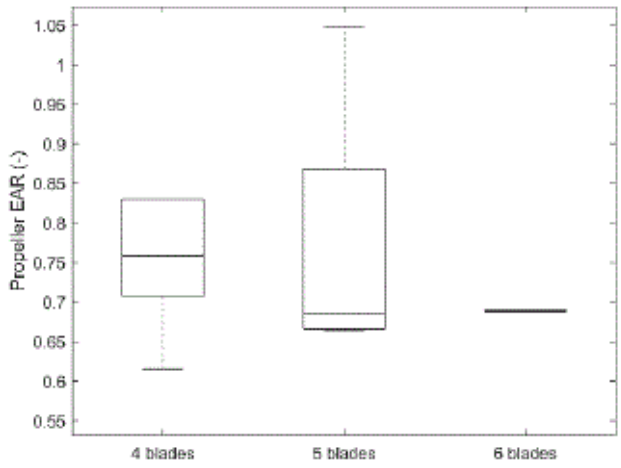

Figure 8. Box plot of EAR among different propeller blades.

the inclined shaft angle; for instance, when there is no inclination, the simulation case is called case 0, and when the inclination angle is 1, then the simulation case is called case 1 and so on. All the propellers are designed to provide the same thrust at the given ship speed no changes are detected for the computed values of wake fraction and thrust deduction fraction, as shown in Table 6.

From the following figures, it has been shown that the optimizer always tries to find the optimum propeller design at the maximum propeller diameter despite all the optimisation constraints. From figures 5 and 6, the difference between propeller diameters is not exceeding 2 cm among the different propeller blades. The minimum propeller diameter is achieved at the higher number of propeller blades (five and six blades), as shown in Figure 6. This increment in propeller diameter in all cases plays an important role in increasing the propeller efficiency as well as providing a sufficient propeller thrust.

The *EAR* is also an important parameter balanced to increase propeller efficiency and avoid cavitation problems; therefore, the simulation is forced to minimize the *EAR* while keeping it greater than the minimum *EAR* as calculated using the Keller method to prevent cavitation. A small *EAR* variation is detected in some cases (1 and 2) along the different blades, as shown in Figure 7, while in Figure 8, the values of the *EAR* are shown the minimum level at four-bladed propellers followed by the five-bladed then the six-bladed propellers. A very small variation in the EAR for all propellers with six blades has been noticed.

Finding a balanced propeller pitch diameter ratio is also an effective way to improve propulsive efficiency. It has been seen from figures 9 and 10 that the value of pitch diameter ratio exceeds 1 in most of the cases; also, it decreases with the increase of blade numbers and in case 2, the pitch diameter ratio shows its lowest levels.

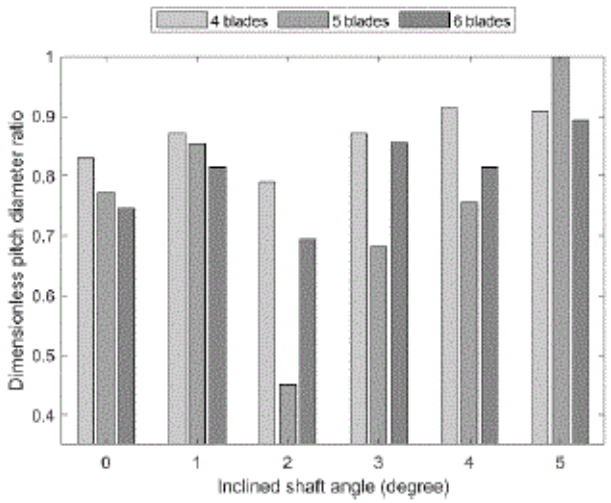

Figure 9. Dimensionless pitch diameter ratio of different propeller blades at several inclined shaft angles.

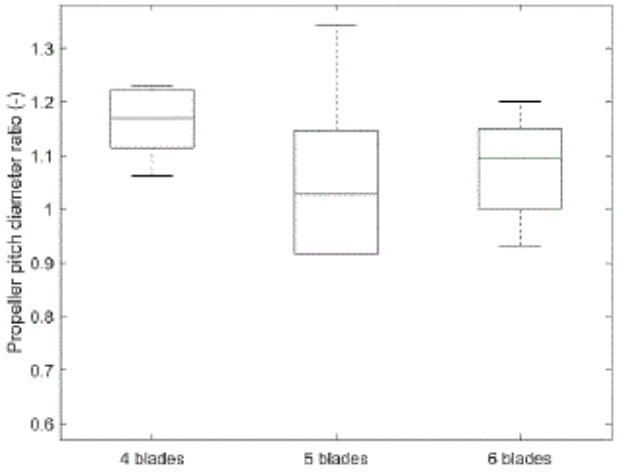

Figure 10. Box plot of pitch diameter ratio among different propeller blades.

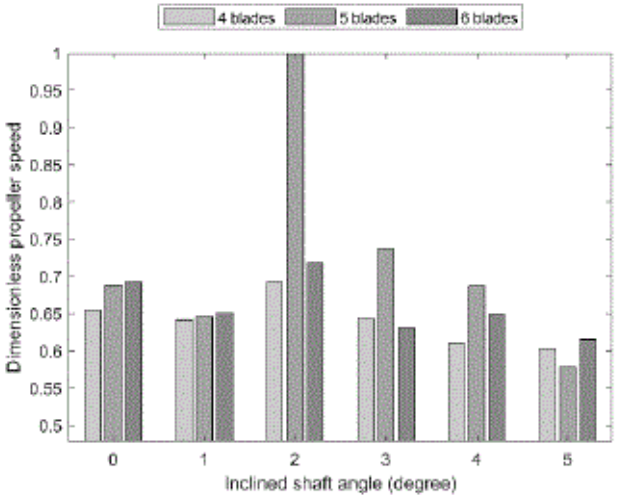

Figure 11. Dimensionless propeller speed of different propeller blades at several inclined shaft angles.

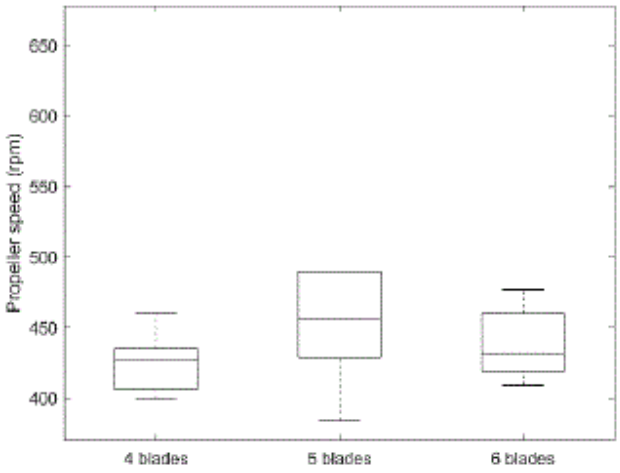

Figure 12. Box plot of propeller speed among different propeller blades.

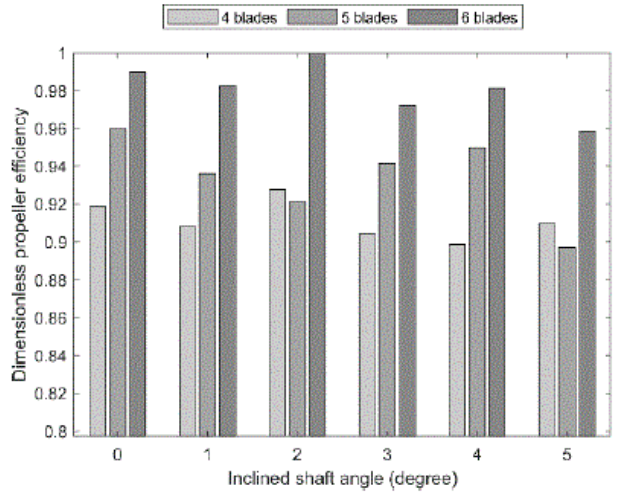

Figure 13. Dimensionless propeller efficiency of different propeller blades at several inclined shaft angles.

In figures 11 and 12, the propeller speed increase with the increase of propeller blades, which leads to a lower in the values of gearbox ratios as in figures 15 and 16. This inverse proportional relation is attained due to the consideration of the same engine load diagram among the simulation cases.

By combining the higher propeller diameters and lower propeller speeds, higher propeller efficiencies are realized in cases with higher propeller blades, as shown in figures 13 and 14.

From figures 17 and 18, up to 20% difference in most of the cases, except in case 2, is achieved between the different advance coefficients, which varies between 0.4 and 0.53. Similarly, the thrust and torque coefficients follow the same trend as the advance coefficient shown in figures 19 to 22.

While the optimized propellers among the different propeller blades comply with the limitations of cavitation,

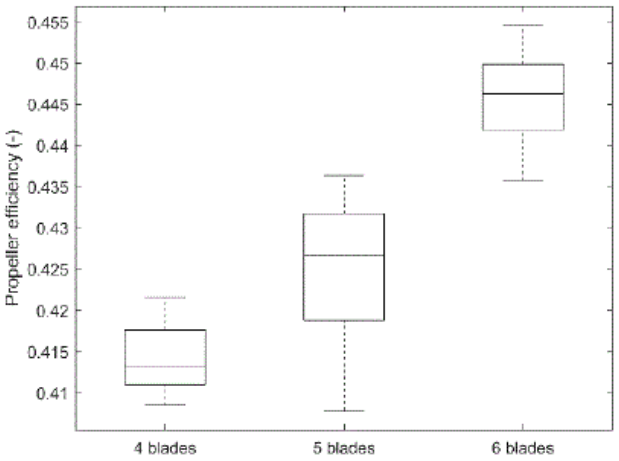

Figure 14. Box plot of propeller efficiency among different propeller blades.

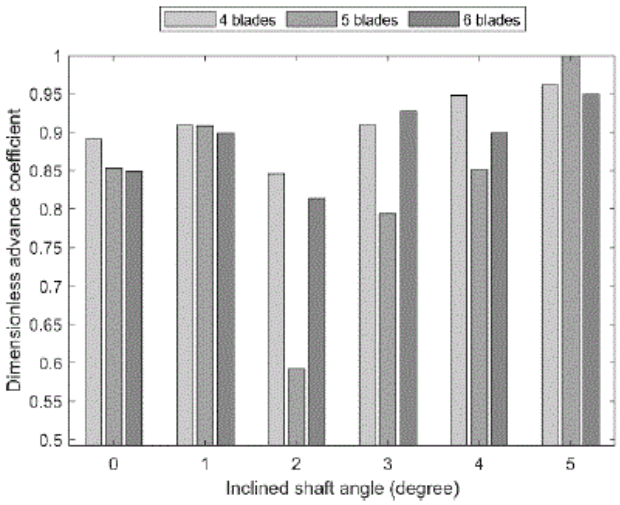

Figure 17. Dimensionless advance coefficient of different propeller blades at several inclined shaft angles.

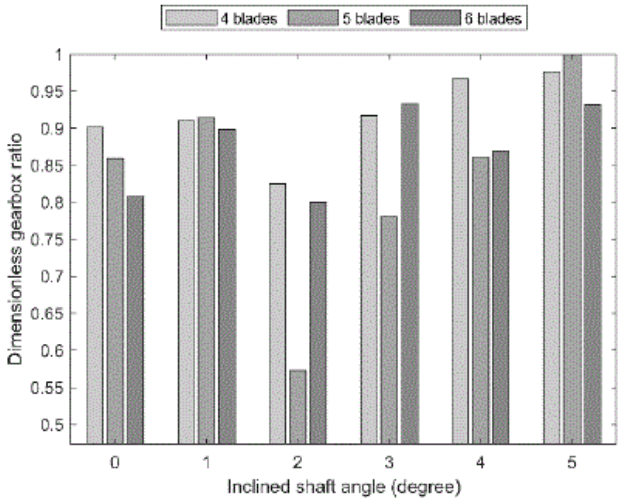

Figure 15. Dimensionless gearbox ratio of different propeller blades at several inclined shaft angles.

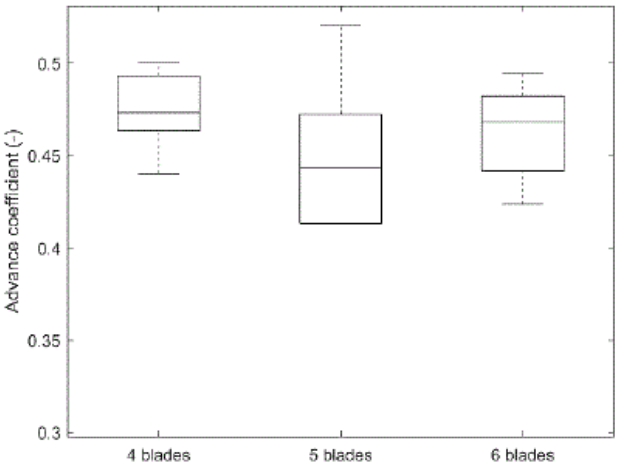

Figure 18. Box plot of advance coefficient among different propeller blades.

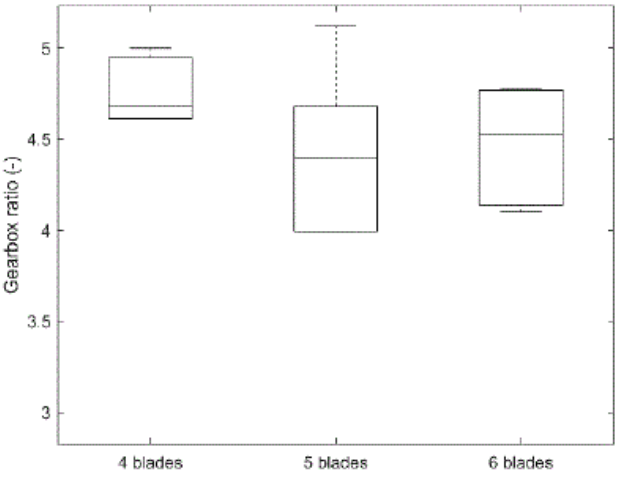

Figure 16. Box plot of gearbox ratio among different propeller blades.

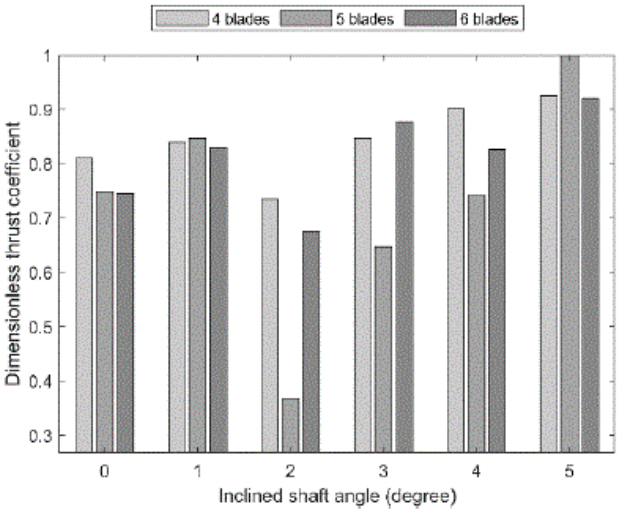

Figure 19. Dimensionless thrust coefficient of different propeller blades at several inclined shaft angles.

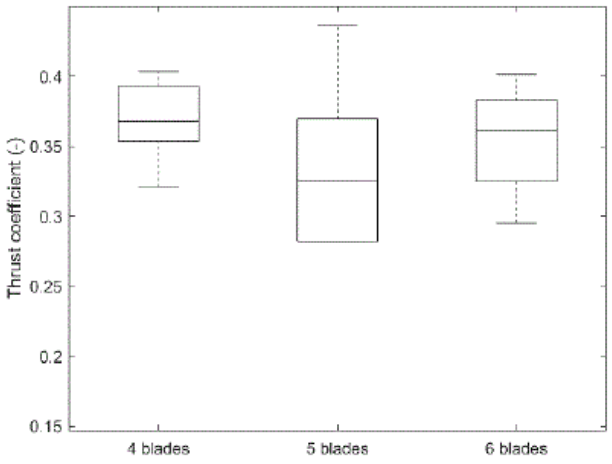

Figure 20. Box plot of thrust coefficient among different propeller blades.

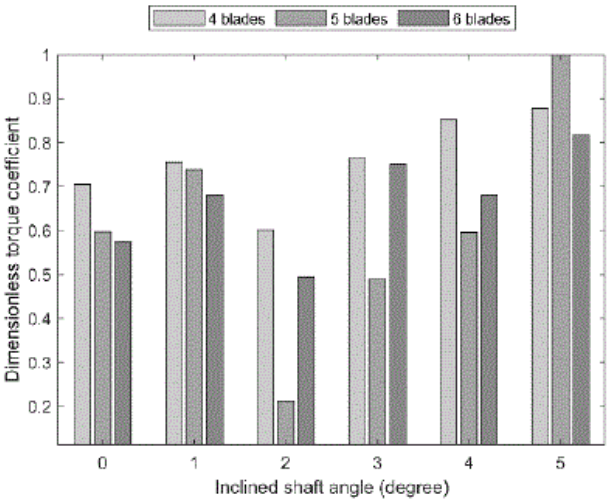

Figure 21. Dimensionless torque coefficient of different propeller blades at several inclined shaft angles.

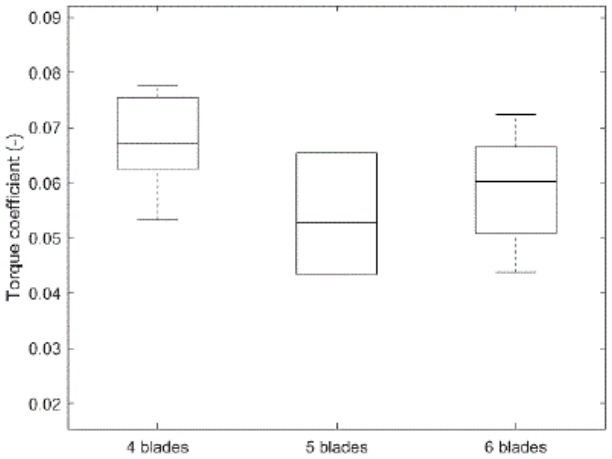

Figure 22. Box plot of torque coefficient among different propeller blades.

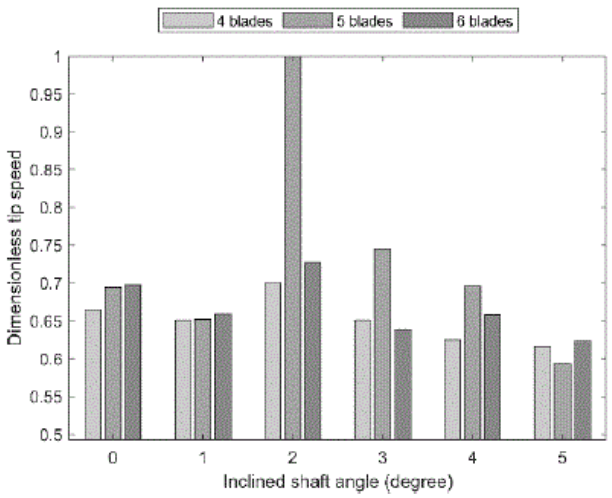

Figure 23. Dimensionless tip speed of different propeller blades at several inclined shaft angles.

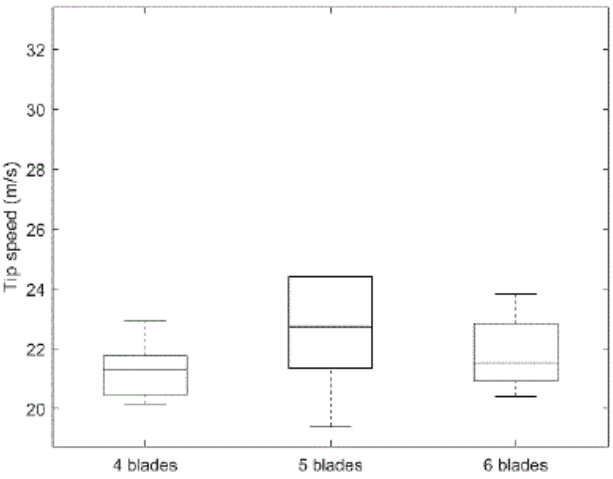

Figure 24. Box plot of tip speed among different propeller blades.

the four-bladed propellers show the lowest values of propeller tip speed than in five- and six-bladed propellers due to the significant reduction in propeller speed, as shown in figures 23 and 24. By increasing the inclined shaft angle, the values of the tip speed decrease among the different blades. The balanced values of both propeller speeds, *EAR* and wake fraction, lead to reduce computed results of average loading pressure. Figures 25 and 26 show that the four-and five-bladed propeller shows the lowest values of average loading pressure, while there is a small variation in the six-bladed propeller. Figures 27 and 28 present the average back cavitation percentage values. The values are lower than the maximum limit provided by the design criterion, which is 15%. It has been shown that the concentration of the values is almost similar in four- and six-bladed propellers while it is higher in five-bladed propellers.

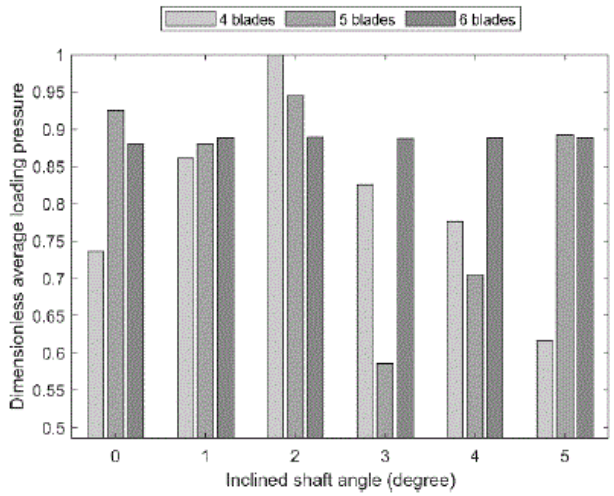

Figure 25. Dimensionless average propeller loading pressure of different propeller blades at several inclined shaft angles.

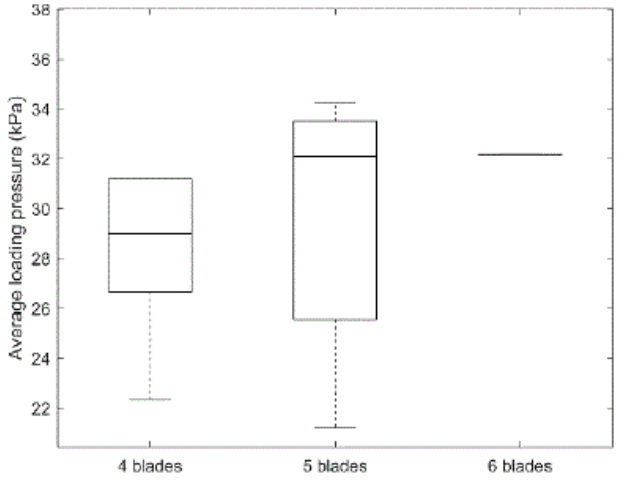

Figure 26. Box plot of average propeller loading pressure among different propeller blades.

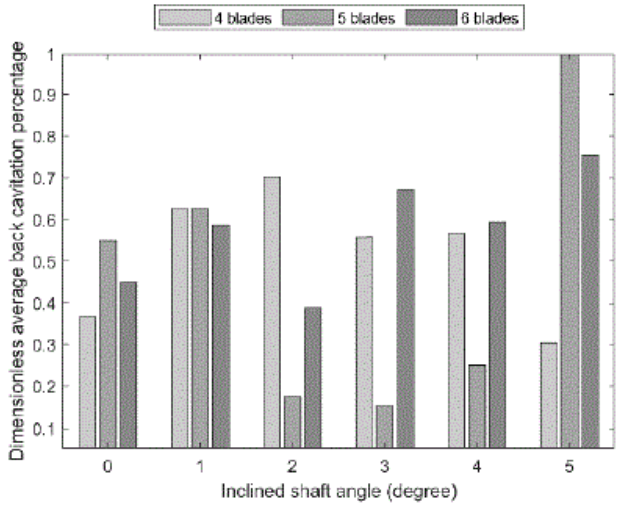

Figure 27. Dimensionless average back cavitation percentage of different propeller blades at several inclined shaft angles.

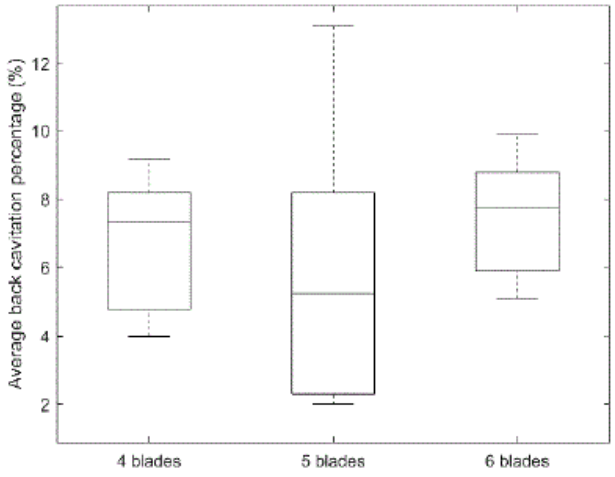

Figure 28. Box plot of average back cavitation percentage among different propeller blades.

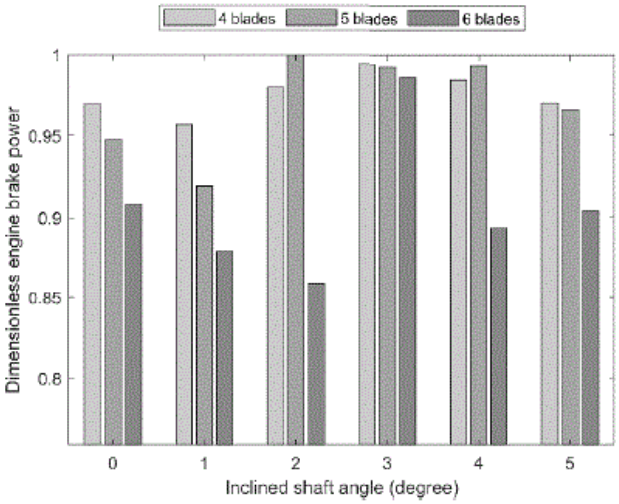

Figure 29. Dimensionless engine brake power of different propeller blades at several inclined shaft angles.

According to the propeller geometry and the operational point mentioned above, the six-bladed propellers show that they can operate at lower engine brake power than the four- and five-bladed propellers by up to 14%, as shown in figures 29 and 30. While the difference between the *BSFC* is not exceeding the 1% between the whole cases as in figures 31 and 32, a significant reduction by up to 0.4 l/nm (approximately 10%) in fuel consumption is detected when considering the higher number of propeller blades as shown in figures 33 and 34.

From all of the cumulative computed results, the optimized six-bladed propeller at 2 degrees inclined propeller shaft consumes less fuel than the other simulated cases and is equal to the horizontal propeller shaft.

This fast numerical model-based optimisation technique shows the ability to optimize the propeller geometry, the

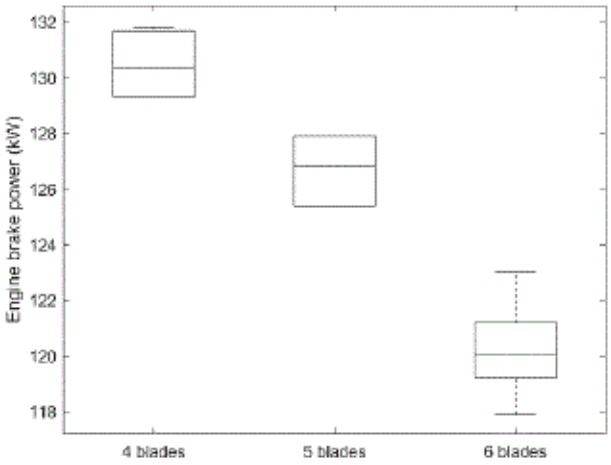

Figure 30. Box plot of engine brake power among different propeller blades.

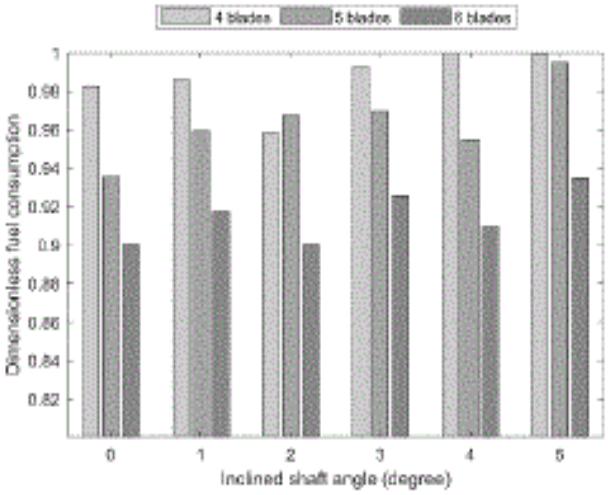

Figure 33. Dimensionless fuel consumption of different propeller blades at several inclined shaft angles.

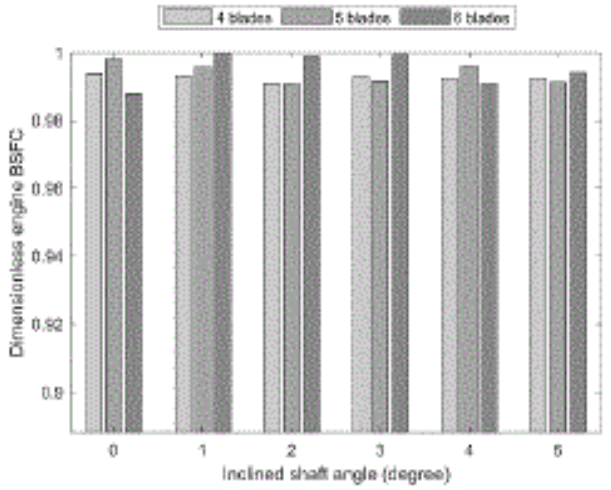

Figure 31. Dimensionless engine BSFC of different propeller blades at several inclined shaft angles.

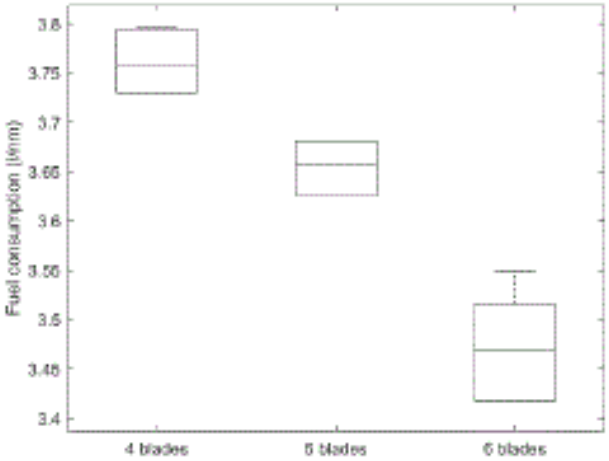

Figure 34. Box plot of fuel consumption among different propeller blades.

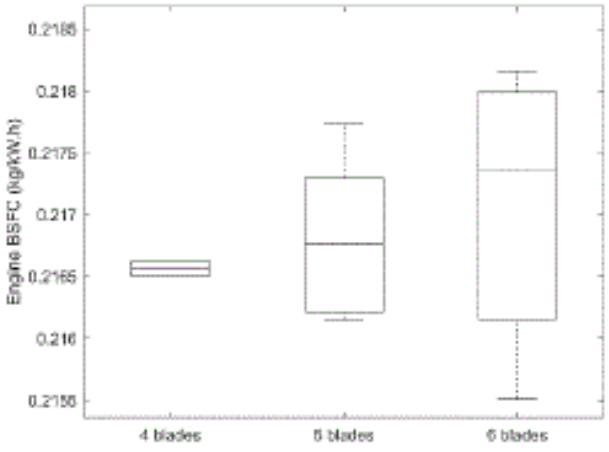

Figure 32. Box plot of engine BSFC percentage among different propeller blades.

operational point, and the inclined angle of the propeller shaft for given propeller blades. This model can be used during the preliminary stage of ship design that requires an inclined propeller shaft according to the needs.

5. CONCLUSIONS

This paper presents a propeller optimisation model, smoothly coupling NavCad and Matlab through API to optimize the propeller performance at the engine operating point with minimum fuel consumption. The computed results of the optimized propeller performance with different propeller blades and different inclined angles of the propeller shaft are analyzed using dimensionless bar chart and box- and whisker plot techniques to have a wide overview of the optimum propeller performance.

It has been concluded that:

1. The propeller performance is computed in a reasonable simulation time.
2. The propeller with a higher number of blades can operate at lower engine brake power, thus consuming lower fuel consumption.
3. The propeller optimisation model shows effectiveness to select the propeller at a larger propeller diameter and lower propeller speed, achieving the best propeller performance.
4. The propeller optimisation model can be able to optimize any propeller for a given vessel at any inclination angle of the propeller shaft during the preliminary stage sof ship design and comply with the different applied constraints.
5. Considering an inclined propeller shaft can be more effiecint in terms of fuel concumption as in the case of 4 blades with 2 degrees compared to the horizontal propeller shaft.
6. Optimized propeller with a higher number of blades at an inclined propeller shaft with 2 degrees can achieve the same fuel consumption when the propeller is optimized at the horizontal propeller shaft. It is suitable for small and medium ships that require an inclined propeller shaft.
7. This study opens the door to consider the inclination angle of the propeller shaft during ship design to achieve more reduction in the fuel consumed.

The model's performance can be extended by comparing the optimized propeller performance with CFD calculations to achieve higher accuracy in wake fraction as well as considering several propeller series to ensure the best performance of the marine system.

6. ACKNOWLEDGEMENTS

This work was performed within the scope of the Strategic Research Plan of the Centre for Marine Technology and Ocean Engineering (CENTEC), which is financed by the Portuguese Foundation for Science and Technology (Fundação para a Ciência e Tecnologia-FCT) under contract UIDB/UIDP/00134/2020.

7. REFERENCES

1. ABS (2021). *Guidance notes on ship vibration*. Texas: American Bureau of Shipping.
2. AKTAS, B., ATLAR, M., TURKMEN, S., KORKUT, E. & FITZSIMMONS, P., (2016). *Systematic cavitation tunnel tests of a Propeller in uniform and inclined flow conditions as part of a round robin test campaign*. Ocean Engineering, 120, 136–151. https://doi.org/10.1016/j.oceaneng.2015.12.015.
3. ALTOSOLE, M., BENVENUTO, G., CAMPORA, U., LAVIOLA, M. & ZACCONE, R., (2017). *Simulation and performance comparison between diesel and natural gas engines for marine applications*. Proceedings of the Institution of Mechanical Engineers, Part M: Journal of Engineering for the Maritime Environment, 231, 690–704. https://doi.org/10.1177/1475090217690964.
4. ANSYS. (2018). *Ansys: Engineering Simulation & 3D Design Software* [Online]. Available: https://www.ansys.com/ (Accessed 15 March 2018).
5. ARAPAKOPOULOS, A., POLICHSHUK, R., SEGIZBAYEV, Z., OSPANOV, S., GINNIS, A. I. & KOSTAS, K. V., (2019). *Parametric models for marine propellers*. Ocean Engineering, 192, 106595. https://doi.org/10.1016/j.oceaneng.2019.106595.
6. BACCIAGLIA, A., CERUTI, A. & LIVERANI, A., (2021). *Controllable pitch propeller optimization through meta-heuristic algorithm*. Engineering with Computers, 37, 2257–2271. https://www.doi.org/10.1007/s00366-020-00938–8.
7. BEKHIT, A. S. & LUNGU, A., (2019). *Simulation of the POW performance of the JBC propeller*. AIP Conference Proceedings, 2116, 450007. https://doi.org/10.1063/1.5114474.
8. BEKHIT, A. S., PACURARUA, F. & PACURARU, S., (2020). *Hull-propeller-rudder interaction of the JBC ship model*. AIP Conference Proceedings, 2293, 420091. https://doi.org/10.1063/5.0027325.
9. BENINI, E., (2003). *Multiobjective design optimization of B-screw series propellers using evolutionary algorithms*. Mar Technol, 40, 229-238. https://doi.org/10.5957/mt1.2003.40.4.229.
10. BLOUNT, D. L. & FOX, D. L., (1978). *Design Considerations for Propellers in a Cavitating Environment*. Marine Technology, 15, 144–178. https://www.doi.org/10.5957/mt1.1978.15.2.144.
11. BURRILL, L. C. & EMERSON, A., (1963). *Propeller cavitation: Further tests on 16in. propeller models in the King's College cavitation tunnel*. International Shipbuilding Progress, 10, 119–131. https://www.doi.org/10.3233/isp-1963-1010402
12. CAESES. (2021). *CAESES* [Online]. Available: https://www.caeses.com/products/caeses/ (Accessed 2 February 2021).
13. CARLTON, J. (2012). *Marine Propellers and Propulsion,* Oxford, Butterworth-Heinemann.
14. DANG, J., BROUWER, J., BOSMAN, R. & POUW, C. (2012). *Quasi-Steady Two-Quadrant Open Water Tests for the Wageningen Propeller C- and D-Series*. *Twenty-Ninth Symposium on Naval Hydrodynamics.* Gothenburg, Sweden.
15. EKINCI, S., (2011). *A Practical Approach for Design of Marine Propellers with Systematic*

Propeller Series. Brodogradnja, 62, 123-129. https://hrcak.srce.hr/71507.

16. ELKAFAS, A. G., ELGOHARY, M. M. & SHOUMAN, M. R., (2021). *Numerical analysis of economic and environmental benefits of marine fuel conversion from diesel oil to natural gas for container ships*. Environmental Science and Pollution Research, 28, 15210–15222. https://www.doi.org/10.1007/s11356-020-11639-6.
17. ELKAFAS, A. G. & SHOUMAN, M. R., (2021). *Assessment of Energy Efficiency and Ship Emissions from Speed Reduction Measures on a Medium Sized Container Ship*. International Journal of Maritime Engineering, 163, 121–132. https://doi.org/10.5750/ijme.v163iA3.805.
18. EPPS, B. P., STANWAY, M. J. & KIMBALL, R. W. (2009). *OpenProp: An Open-source Design Tool for Propellers and Turbines*. *SNAME Propellers and Shafting Symposium.* Williamsburg, VA, USA.
19. GAAFARY, M. M., EL-KILANI, H. S. & MOUSTAFA, M. M., (2011). *Optimum design of B-series marine propellers*. Alexandria Engineering Journal, 50, 13–18. https://doi.org/10.1016/j.aej.2011.01.001.
20. GAGGERO, S., TANI, G., VILLA, D., VIVIANI, M., AUSONIO, P., TRAVI, P., BIZZARRI, G. & SERRA, F., (2017). *Efficient and multi-objective cavitating propeller optimization: An application to a high-speed craft*. Applied Ocean Research, 64, 31–57. https://doi.org/10.1016/j.apor.2017.01.018.
21. GAGGERO, S. & VILLA, D., (2018). *Cavitating Propeller Performance in Inclined Shaft Conditions with OpenFOAM: PPTC 2015 Test Case*. Journal of Marine Science and Application, 17, 1–20. https://www.doi.org/img/banner-413.gif10.1007/s11804-018-0008-6.
22. GAGGERO, S., VILLA, D. & BRIZZOLARA, S., (2010). *RANS and PANEL method for unsteady flow propeller analysis*. Journal of Hydrodynamics, Ser. B, 22, 564–569. https://doi.org/10.1016/S1001-6058(09)60253-5.
23. GHAEMI, M. H. & ZERAATGAR, H., (2021). *Analysis of hull*, *propeller and engine interactions in regular waves by a combination of experiment and simulation*. Journal of Marine Science and Technology, 26, 257–272. https://doi.org/10.1007/s00773-020-00734-5.
24. HELICIEL. (2019). *Propellers Software design screw Calculator boats, aerial, wings, hydrofoils* [Online]. Available: https://heliciel.com/en/logiciel-calcul-helice-aile/Logiciel%20calcul%20helices%20et%20ailes%20Heliciel.htm (Accessed 9 September 2021).
25. HOLTROP, J., (1984). *A statistical re-analysis of resistance and propulsion data*. International Shipbuilding Progress, 31, 272–276.
26. HOLTROP, J. (1988). *A Statistical Resistance Prediction Method With a Speed Dependent Form Factor*. *Proceedings of Scientific and Methodological Seminar on Ship Hydrodynamics (SMSSH '88).* Varna: Bulgarian Ship Hydrodynamics Centre, pp. 1–7.
27. HOLTROP, J. & MENNEN, G. G. J., (1982). *An approximate power prediction method*. International Shipbuilding Progress, 29, 166-170.
28. HYDROCOMP. (2018). *NavCad: Reliable and Confident Performance Prediction* [Online]. HydroComp Inc. Available: https://www.hydrocompinc.com/solutions/navcad/ (Accessed 30 January 2019).
29. ISLAM, H., VENTURA, M., GUEDES SOARES, C., TADROS, M. & ABDELWAHAB, H. S. (2022). *Comparison between empirical and CFD based methods for ship resistance and power prediction*. *In:* Guedes Soares, C. & Santos, T. A. (eds.) *Trends in Maritime Technology and Engineering.* London: Taylor & Francis Group, pp. 347–357.
30. ITTC (2008). *Proceedings of the 25th ITTC.* Fukuoka, Japan: The Japan Society of Naval Architects and Ocean Engineers.
31. KAEWKHIAW, P., (2020). *CFD analysis of unsteady propeller performance operating at different inclined shaft angles for long-tail boat in Thailand*. Journal of Naval Architecture and Marine Engineering, 17. http://dx.doi.org/10.3329/jname.v17i2.42622.
32. KIM, S. & KINNAS, S. A., (2020). *Prediction of Unsteady Developed Tip Vortex Cavitation and Its Effect on the Induced Hull Pressures*. Journal of Marine Science and Engineering, 8, 114. https://www.doi.org/10.3390/jmse8020114.
33. KUMAR, A., VIJAYAKUMAR, R. & SUBRAMANIAN, V., (2021). *Numerical Fluid-Structure Interaction Analysis for a Flexible Marine Propeller Using Co-Simulation Method*. International Journal of Maritime Engineering, 163,81-89.https://doi.org/10.5750/ijme.v163iA2.759.
34. LEE, C.-S., CHOI, Y.-D., AHN, B.-K., SHIN, M.-S. & JANG, H.-G., (2010). *Performance optimization of marine propellers*. International Journal of Naval Architecture and Ocean Engineering, 2, 211-216. https://doi.org/10.2478/IJNAOE-2013-0038.
35. MACPHERSON, D., HARRIES, S., BROENSTRUP, S. & DUDKA, J. (2016). *Real cost savings for a waterjet-driven patrol craft design using a CAESES-NavCad coupled solution*. *15th computer applications and information technology in the maritime industries (COMPIT 2016).* Lecce, Italy.
36. MAN ENERGY SOLUTIONS. (2020). *Propulsion: MAN Alpha propeller & aft ship*

solutions [Online]. Augsburg, Germany. Available: https://www.man-es.com/marine/products/propeller-aft-ship (Accessed 01 July 2021).
37. MARIN. (2020). *Propeller design and analysis* [Online]. Available: https://www.marin.nl/en/facilities-and-tools/software (Accessed 9 September 2021).
38. MCGILL, R., TUKEY, J. W. & LARSEN, W. A., (1978). *Variations of Boxplots*. The American Statistician, 32, 12-16.
39. MIRJALILI, S., LEWIS, A. & MIRJALILI, S. A. M., (2015). *Multi-objective Optimisation of Marine Propellers*. Procedia Computer Science, 51, 2247–2256. https://doi.org/10.1016/j.procs.2015.05.504.
40. NOURI, N. M., MOHAMMADI, S. & ZAREZADEH, M., (2018). *Optimization of a marine contra-rotating propellers set*. Ocean Engineering, 167, 397–404. https://doi.org/10.1016/j.oceaneng.2018.05.067.
41. OOSTERVELD, M. & VAN OOSSANEN, P., (1975). *Further computer-analyzed data of the Wageningen B-screw series*. International Shipbuilding Progress, 22.
42. OOSTERVELD, M. W. C. (1970). *Wake Adapted Ducted Propellers.* Doctoral Thesis, Delft University of Technology.
43. PAIK, B.-G., KIM, K.-S., KIM, K.-Y., AHN, J.-W., KIM, T.-G., KIM, K.-R., JANG, Y.-H. & LEE, S.-U., (2011). *Test method of cavitation erosion for marine coatings with low hardness*. Ocean Engineering, 38, 1495–1502. https://doi.org/10.1016/j.oceaneng.2011.07.008.
44. PECK, J. G. (1974). *Performance Characteristics Of Three Propellers With Varying Pitch Distributions On An Inclined Shaft*. Springfield, Virginia: Naval Sea Systems Command.
45. PECK, J. G. & MOORE, D. H., (1973). *Inclined-Shaft Propeller Performance Characteristics*. SNAME Spring Meeting / STAR Papers.
46. PLUCIŃSKI, M. M., YOUNG, Y. L. & LIU, Z. (2007). *Optimization of a self-twisting composite marine propeller using genetic algorithms*. *16th international conference on composite materials.* Japan.
47. RADOJČIĆ, D. (1985). *Optimal preliminary propeller design using nonlinear constrained mathematical programming technique*. Southampton: University of Southampton.
48. SEYYEDI, S. M., SHAFAGHAT, R. & SIAVOSHIAN, M., (2019). *Experimental study of immersion ratio and shaft inclination angle in the performance of a surface-piercing propeller*. Mech. Sci., 10, 153–167. https://www.doi.org/10.5194/ms-10-153-2019.
49. SILVESTRE, M. A., MORGADO, J. P. & PASCOA, J. (2013). *JBLADE: A propeller design and analysis code*. *2013 International Powered Lift Conference.* Los Angeles, CA.
50. SOLÉ DIESEL. (2021). *Solé Diesel marine engine SDZ-280* [Online]. Available: https://www.solediesel.com/en/sole-diesel-marine-engine-sdz-280-fa1086 (Accessed 05 January 2021).
51. SUEN, J.-B. & KOUH, J.-S. (1999). *Genetic algorithms for optimal series propeller design*. *Proceedings of the third international conference on marine technology.* Szczecin, Poland: WIT press.
52. TADROS, M., VENTURA, M. & GUEDES SOARES, C. (2018a). *Optimization scheme for the selection of the propeller in ship concept design*. *In:* Guedes Soares, C. & Santos, T. A. (eds.) *Progress in Maritime Technology and Engineering.* London: Taylor & Francis Group, pp. 233–239.
53. TADROS, M., VENTURA, M. & GUEDES SOARES, C. (2018b). *Surrogate models of the performance and exhaust emissions of marine diesel engines for ship conceptual design*. *In:* Guedes Soares, C. & Teixeira, A. P. (eds.) *Maritime Transportation and Harvesting of Sea Resources.* London: Taylor & Francis Group, pp. 105–112.
54. TADROS, M., VENTURA, M. & GUEDES SOARES, C., (2019). *Optimization procedure to minimize fuel consumption of a four-stroke marine turbocharged diesel engine*. Energy, 168, 897–908. https://doi.org/10.1016/j.energy.2018.11.146.
55. TADROS, M., VENTURA, M. & GUEDES SOARES, C., (2020a). *Data Driven In-Cylinder Pressure Diagram Based Optimization Procedure*. Journal of Marine Science and Engineering, 8, 294. https://www.doi.org/10.3390/jmse8040294.
56. TADROS, M., VENTURA, M. & GUEDES SOARES, C., (2020b). *A nonlinear optimization tool to simulate a marine propulsion system for ship conceptual design*. Ocean Engineering, 210, 1-15. https://doi.org/10.1016/j.oceaneng.2020.107417.
57. TADROS, M., VENTURA, M. & GUEDES SOARES, C., (2020c). *Optimization of the performance of marine diesel engines to minimize the formation of SOx emissions*. Journal of Marine Science and Application, 19, 473–484. https://www.doi.org/10.1007/s11804-020-00156-0.
58. TADROS, M., VENTURA, M. & GUEDES SOARES, C., (2021a). *Design of Propeller Series Optimizing Fuel Consumption and Propeller Efficiency*. Journal of Marine Science and Engineering, 9, 1226. https://doi.org/10.3390/jmse9111226.
59. TADROS, M., VENTURA, M. & GUEDES SOARES, C. (2021b). *A review of the use of Biodiesel as a green fuel for diesel engines*. *In:* Guedes Soares, C. & Santos, T. (eds.) *Developments*

in Maritime Technology and Engineering. London: Taylor & Francis Group, pp. 481–490.

60. TADROS, M., VETTOR, R., VENTURA, M. & GUEDES SOARES, C., (2021c). *Coupled Engine-Propeller Selection Procedure to Minimize Fuel Consumption at a Specified Speed*. Journal of Marine Science and Engineering, 9, 59. https://doi.org/10.3390/jmse9010059.
61. TADROS, M., VETTOR, R., VENTURA, M. & GUEDES SOARES, C. (2022a). *Effect of different speed reduction strategies on ship fuel consumption in realistic weather conditions*. *In:* Guedes Soares, C. & Santos, T. A. (eds.) *Trends in Maritime Technology and Engineering.* London: Taylor & Francis Group, pp. 553–561.
62. TADROS, M., VETTOR, R., VENTURA, M. & GUEDES SOARES, C., (2022b). *Effect of propeller cup on the reduction of fuel consumption in realistic weather conditions*. Journal of Marine Science and Engineering, 10, 1039. https://doi.org/10.3390/jmse10081039.
63. TAHERI, R. & MAZAHERI, K., (2013). *Hydrodynamic Optimization of Marine Propeller Using Gradient and Non-Gradientbased Algorithms*. Acta Polytechnica Hungarica, 10. https://www.doi.org/10.12700/aph.10.03.2013.3.15.
64. TAN, Y., LI, J., LI, Y. & LIU, C., (2019). *Improved Performance Prediction of Marine Propeller: Numerical Investigation and Experimental Verification*. Mathematical Problems in Engineering, Vol. 2019, Article ID 7501524, 10. https://doi.org/10.1155/2019/7501524.
65. THE MATHWORKS INC. (2018). *Constrained Nonlinear Optimization Algorithms* [Online]. Available: https://www.mathworks.com/help/optim/ug/constrained-nonlinear-optimization-algorithms.html (Accessed 03 February 2018).
66. USTA, O. & KORKUT, E., (2018). *A study for cavitating flow analysis using DES model*. Ocean Engineering, 160, 397–411. https://doi.org/10.1016/j.oceaneng.2018.04.064.
67. VAN LAMMEREN, W. P. A., VAN MANEN, J. D. & OOSTERVELD, M. W. C., (1969). *The Wageningen B-screw series*. Trans. SNAME, 77, 269–317.
68. VESTING, F. & BENSOW, R. (2011). *Propeller Optimisation Considering Sheet Cavitation and Hull Interaction*. *Second International Symposium on Marine Propulsors (smp'11).* Hamburg, Germany.
69. VETTOR, R. & GUEDES SOARES, C., (2015). *Detection and Analysis of the Main Routes of Voluntary Observing Ships in the North Atlantic*. Journal of Navigation, 68, 397-410. https://www.doi.org/10.1017/S0373463314000757.
70. VETTOR, R. & GUEDES SOARES, C., (2016). *Development of a ship weather routing system*. Ocean Engineering, 123, 1-14. http://dx.doi.org/10.1016/j.oceaneng.2016.06.035.
71. VETTOR, R., TADROS, M., VENTURA, M. & GUEDES SOARES, C. (2016). *Route planning of a fishing vessel in coastal waters with fuel consumption restraint*. *In:* Guedes Soares, C. & Santos, T. A. (eds.) *Maritime Technology and Engineering 3.* London: Taylor & Francis Group, pp. 167-173.
72. VLAŠIĆ, D., DEGIULI, N., FARKAS, A. & MARTIĆ, I., (2018). *The preliminary design of a screw propeller by means of computational fluid dynamics*. Brodogradnja, 69, 129-147. https://doi.org/10.21278/brod69308.
73. WÄRTSILÄ. (2021). *Propellers Efficiency and manoeuvrability improvements* [Online]. Helsinki, Finland. Available: https://www.wartsila.com/marine/build/propulsors-and-gears/propellers (Accessed 01 July 2021).
74. YE, L. Y., GUO, C. Y., WANG, C., WANG, C. H. & CHANG, X., (2019). *Strength assessment method of ice-class propeller under the design ice load condition*. International Journal of Naval Architecture and Ocean Engineering, 11, 542-552. https://doi.org/10.1016/j.ijnaoe.2018.09.008.
75. ZALACKO, R., ZÖLDY, M. & SIMONGÁTI, G., (2021). *Comparison of alternative propulsion systems - a case study of a passenger ship used in public transport*. Brodogradnja, 72, 1–18. https://doi.org/10.21278/brod72201.

APPENDIX

Table 5: Performance of optimized propellers at different initial starting point.

Initial start			LB	(LB+UB)/4	(LB+UB)/2	(LB+UB)*3/4	UB	Rand
Propeller type			BSeries	BSeries	BSeries	BSeries	BSeries	BSeries
Propeller characteristics	**Number of Blades**	[-]	6	6	6	6	6	6
	Inclined Angle	[degree]	0	0	0	0	0	0
	Thrust	[kN]	15.9	15.9	15.9	15.9	15.9	15.9
	Torque	[kN.m]	1.88	2.43	2.37	2.35	2.85	2.23
	Speed	[RPM]	585	447	455	460	397	491
	D	[m]	0.95	0.95	0.95	0.95	0.96	0.95
	EAR	[-]	0.69	0.74	0.70	0.70	0.73	0.78
	P	[m]	0.66	0.98	0.96	0.95	1.19	0.86
	P/D	[-]	0.69	1.03	1.01	1.00	1.25	0.91
	η_0	[%]	44	45	45	45	43	44
	J	[-]	0.35	0.45	0.44	0.44	0.51	0.42
	KT	[-]	0.20	0.34	0.33	0.32	0.42	0.29
	KQ	[-]	0.02	0.05	0.05	0.05	0.08	0.04
	w	[-]	0.306	0.306	0.306	0.306	0.306	0.306
	t	[-]	0.226	0.226	0.226	0.226	0.226	0.226
Cavitation	**Tip Speed**	[m/s]	29.15	22.29	22.68	22.84	19.86	24.31
	EAR_{min}	[-]	0.69	0.69	0.69	0.69	0.69	0.70
	Average loading pressure	[kPa]	32.19	30.14	31.77	31.86	30.15	29.10
	Back Cavitation	[%]	2.5	5.5	6.0	5.9	9.2	3.5
Gearbox characteristics	**GBR**	[-]	3.27	4.27	4.38	4.14	5.12	4.09
Engine characteristics	**Speed**	[RPM]	1914	1911	1994	1902	2030	2008
	Brake Power	[kW]	121.20	120.40	119.00	119.20	124.70	121.20
	Loading ratio	[%]	0.61	0.60	0.60	0.60	0.62	0.61
	BSFC	[g/kW.h]	215.73	215.72	218.37	215.51	217.15	217.95
	Fuel consumption	[l/nm]	3.48	3.46	3.46	3.42	3.60	3.52

Table 6. Performance of optimized propellers at different blades and Inclined shaft angle.

Propeller type			BSeries	BSeries	BSeries	BSeries	BSeries	BSeries
Propeller characteristics	Number of Blades	[-]	4	4	4	4	4	4
	Inclined Angle	[degree]	0	1	2	3	4	5
	Thrust	[kN]	15.8	15.9	15.8	15.8	15.8	15.9
	Torque	[kN.m]	2.67	2.77	2.50	2.76	2.93	2.94
	Speed	[RPM]	435	426	460	427	406	400
	D	[m]	0.95	0.96	0.95	0.95	0.96	0.96
	EAR	[-]	0.83	0.71	0.62	0.74	0.77	0.97
	P	[m]	1.06	1.12	1.01	1.11	1.18	1.18
	P/D	[-]	1.12	1.17	1.06	1.17	1.23	1.22
	η_o	[%]	41.76	41.28	42.16	41.10	40.85	41.36
	J	[-]	0.46	0.47	0.44	0.47	0.49	0.50
	KT	[-]	0.35	0.37	0.32	0.37	0.39	0.40
	KQ	[-]	0.06	0.07	0.05	0.07	0.08	0.08
	w	[-]	0.306	0.306	0.306	0.306	0.306	0.306
	t	[-]	0.226	0.226	0.226	0.226	0.226	0.226
Cavitation	Tip Speed	[m/s]	21.76	21.33	22.92	21.32	20.47	20.17
	EAR_{min}	[-]	0.59	0.59	0.60	0.60	0.59	0.59
	Average loading pressure	[kPa]	26.66	31.19	36.24	29.90	28.12	22.33
	Back Cavitation	[%]	4.8	8.2	9.2	7.3	7.4	4.0
Gearbox characteristics	GBR	[-]	4.61	4.66	4.22	4.70	4.95	5.00
Engine characteristics	Speed	[RPM]	2008	1985	1945	2006	2009	1998
	Brake Power	[kW]	129.30	129.90	126.50	130.80	131.80	131.70
	Loading ratio	[%]	0.65	0.65	0.63	0.65	0.66	0.66
	BSFC	[g/kW.h]	216.78	216.63	216.18	216.61	216.50	216.50
	Fuel consumption	[l/nm]	3.73	3.74	3.64	3.77	3.80	3.79
Simulation time		[s]	1676.69	2760.29	2511.19	1168.45	786.54	752.42

BSeries	BSeries	BSeries	BSeries	BSeries	BSeries	BSeries	BSeries	BSeries	BSeries	BSeries	BSeries
5	5	5	5	5	5	6	6	6	6	6	6
0	1	2	3	4	5	0	1	2	3	4	5
15.9	15.9	15.8	15.9	15.8	15.8	15.9	15.8	15.9	15.9	15.8	15.9
2.44	2.67	1.75	2.33	2.47	3.09	2.35	2.51	2.24	2.63	2.52	2.73
457	429	664	490	456	384	460	432	477	419	431	409
0.95	0.95	0.94	0.95	0.95	0.96	0.95	0.95	0.95	0.95	0.95	0.95
0.67	0.70	0.66	1.05	0.87	0.67	0.70	0.69	0.69	0.69	0.69	0.69
0.99	1.09	0.57	0.87	0.97	1.30	0.95	1.04	0.89	1.10	1.04	1.15
1.04	1.15	0.61	0.92	1.02	1.34	1.00	1.09	0.93	1.15	1.09	1.20
43.64	42.55	41.88	42.80	43.18	40.78	44.99	44.66	45.46	44.19	44.60	43.58
0.44	0.47	0.31	0.41	0.44	0.52	0.44	0.47	0.42	0.48	0.47	0.49
0.33	0.37	0.16	0.28	0.32	0.44	0.32	0.36	0.30	0.38	0.36	0.40
0.05	0.07	0.02	0.04	0.05	0.09	0.05	0.06	0.04	0.07	0.06	0.07
0.306	0.306	0.306	0.306	0.306	0.306	0.306	0.306	0.306	0.306	0.306	0.306
0.226	0.226	0.226	0.226	0.226	0.226	0.226	0.226	0.226	0.226	0.226	0.226
22.73	21.35	32.74	24.41	22.77	19.40	22.84	21.56	23.83	20.92	21.55	20.42
0.65	0.64	0.65	0.64	0.64	0.63	0.69	0.69	0.69	0.69	0.69	0.69
33.52	31.87	34.24	21.22	25.55	32.33	31.86	32.20	32.21	32.16	32.20	32.19
7.2	8.2	2.3	2.0	3.3	13.1	5.9	7.7	5.1	8.8	7.8	9.9
4.40	4.68	2.93	3.99	4.40	5.12	4.14	4.60	4.10	4.77	4.45	4.77
2007	2007	1949	1955	2009	1969	1902	1988	1955	1999	1920	1949
122.60	126.00	127.70	127.90	125.40	131.30	119.20	120.00	117.90	121.20	120.10	123.00
0.61	0.63	0.64	0.64	0.63	0.66	0.60	0.60	0.59	0.61	0.60	0.62
217.73	217.22	216.15	216.30	217.29	216.22	215.51	218.15	217.83	217.99	216.16	216.82
3.55	3.64	3.67	3.68	3.63	3.78	3.42	3.48	3.42	3.52	3.45	3.55
1097.89	2082.21	1896.09	1923.87	3234.71	1085.42	1792.53	924.50	3607.06	1269.62	993.47	2114.81